

# PHARMACEUTICAL NANOTECHNOLOGY

## Polymer-Surfactant Nanoparticles for Sustained Release of Water-Soluble Drugs

MAHESH D. CHAVANPATIL,<sup>1</sup> AYMAN KHDAIR,<sup>1</sup> YOGESH PATIL,<sup>1</sup> HITESH HANDA,<sup>2</sup> GUANGZHAO MAO,<sup>2</sup> JAYANTH PANYAM<sup>1,3</sup>

<sup>1</sup>Department of Pharmaceutical Sciences, Eugene Applebaum College of Pharmacy and Health Sciences, Wayne State University, Detroit, MI 48201

<sup>2</sup>Department of Chemical Engineering and Materials Science, College of Engineering, Wayne State University, Detroit, MI 48202

<sup>3</sup>Karmanos Cancer Institute, Detroit, MI 48201

Received 25 October 2006; revised 19 December 2006; accepted 6 February 2007

Published online in Wiley InterScience (www.interscience.wiley.com). DOI 10.1002/jps.20961

**ABSTRACT:** Poor drug encapsulation efficiency and rapid release of the encapsulated drug limit the use of nanoparticles in biomedical applications involving water-soluble drugs. We have developed a novel polymer-surfactant nanoparticle formulation, using the anionic surfactant Aerosol OT<sup>TM</sup> (AOT) and polysaccharide polymer alginate, for sustained release of water-soluble drugs. Particle size of nanoparticles, as determined by atomic force microscopy and transmission electron microscopy, was in the range of 40–70 nm. Weakly basic molecules like methylene blue, doxorubicin, rhodamine, verapamil, and clonidine could be encapsulated efficiently in AOT-alginate nanoparticles. *In vitro* release studies with basic drug molecules indicate that nanoparticles released 60–70% of the encapsulated drug over 4 weeks, with near zero-order release during the first 15 days. Studies with anionic drug molecules demonstrate poorer drug encapsulation efficiency and more rapid drug release than those observed with basic drugs. Further studies investigating the effect of sodium concentration in the release medium and the charge of the drug suggest that calcium-sodium exchange between nanoparticle matrix and release medium and electrostatic interaction between drug and nanoparticle matrix are important determinants of drug release. In conclusion, we have formulated a novel surfactant-polymer drug delivery carrier demonstrating sustained release of water-soluble drugs. © 2007 Wiley-Liss, Inc. and the American Pharmacists Association *J Pharm Sci* 96:3379–3389, 2007

**Keywords:** alginate; drug delivery; controlled release; nanoparticles; polyelectrolytes; surfactants

### INTRODUCTION

Biodegradable nanoparticles, with a particle size of about 100 nm, have certain unique advantages in drug delivery<sup>1</sup>. Nanoparticles can penetrate

small capillaries, allowing enhanced accumulation of nanoparticle-encapsulated drug at target sites<sup>2</sup>. Nanoparticles can passively target tumor tissue through enhanced permeation and retention effect<sup>3,4</sup>. Nanoparticles can be delivered to distant target sites either by localized catheter-based infusion<sup>5</sup> or by attaching a tissue-specific targeting ligand to nanoparticle surface<sup>6</sup>. Nanoparticles could also be used to encapsulate an imaging agent such as gadolinium<sup>7</sup>. Nanoparticles loaded with

Correspondence to: Jayanth Panyam (Telephone: 612 624 0951; Fax: 612 626 2125; E-mail: jpanyam@umn.edu)

*Journal of Pharmaceutical Sciences*, Vol. 96, 3379–3389 (2007)  
© 2007 Wiley-Liss, Inc. and the American Pharmacists Association

both imaging and therapeutic agents could be used for simultaneous drug delivery and imaging applications.<sup>8</sup>

Nanoparticles fabricated using synthetic polymers such as polylactides<sup>9,10</sup> or polyanhydrides<sup>11</sup> are suitable delivery vehicles for water-insoluble drugs like paclitaxel and dexamethasone, and hydrophilic macromolecules like proteins<sup>12,13</sup> and DNA.<sup>14</sup> However, nanoparticles formulated using synthetic polymers, in general, demonstrate low drug encapsulation efficiency and rapid release of water-soluble drugs. For example, nanoparticles formulated using poly(D,L-lactide-co-glycolide) (PLGA) demonstrated near-complete release of water-soluble sodium phosphate salt of dexamethasone within 8 h.<sup>15</sup> Similarly, polycaprolactone and PLGA nanoparticles demonstrated complete release of a water-soluble drug, propranolol hydrochloride, in 8 h.<sup>16</sup>

Nanoparticles formulated using hydrophilic polymers also show rapid drug release. For example, Yi et al.<sup>17</sup> investigated alginate-bovine serum albumin nanoparticles for 5-fluorouracil. Those nanoparticles released 84% of the encapsulated drug within 72 h. Gelatin nanoparticles were investigated as carriers for methotrexate sodium.<sup>18</sup> The entire drug load was released within 150 h, with a burst release of 40% in the first 10 h. Gelatin nanoparticles were also investigated for sustained delivery of pilocarpine hydrochloride.<sup>19</sup> Depending on the composition, those nanoparticles released about 50–60% of the encapsulated drug in 3 h. In another study, alginate particles released about 70% of encapsulated verapamil hydrochloride in 3 h.<sup>20</sup>

Thus, there is a clear need for nanoparticle formulations that can efficiently encapsulate and sustain the release of water-soluble, small molecular weight drugs. We have developed a novel nanoparticle formulation for water-soluble drugs, using dioctyl sodium sulfosuccinate (Aerosol OT<sup>TM</sup>, (AOT)) and sodium alginate. AOT is an anionic surfactant that is approved as oral, topical, and intramuscular excipient (U.S. Food and Drug Administration's Inactive Ingredients Database). Sodium alginate is a naturally occurring polysaccharide that has been extensively investigated for drug delivery and tissue engineering applications.<sup>21,22</sup> The objectives of the current study were to investigate AOT-alginate nanoparticles for encapsulation and release of water-soluble drugs and study the effect of various formulation parameters on drug encapsulation, and *in vitro* release of the encapsulated drug.

## MATERIALS AND METHODS

### Materials

Doxorubicin, rhodamine 123, verapamil, methylene blue and clonidine (all hydrochloride salts), sodium alginate, polyvinyl alcohol (PVA, 30,000–70,000 Da), and calcium chloride were purchased from Sigma-Aldrich (St. Louis, MO). Fluorescein sodium, diclofenac sodium, AOT, ethanol, and methylene chloride were purchased from Fisher Scientific (Chicago, IL).

### Methods

#### *Nanoparticle Formulation*

Nanoparticles were formulated by emulsion-crosslinking technology developed in our laboratory. Sodium alginate solution in water (0.1%–1.0 % w/v; 1 mL) was emulsified into AOT solution in methylene chloride (0.05–20% w/v; 1–3 mL) by either vortexing (Genie<sup>TM</sup>, Fisher Scientific) or sonication (Model 3000, Misonix, Farmingdale, NY) for 1 min over ice bath. The primary emulsion was further emulsified into 15 mL of aqueous PVA solution (0.5–5% w/v) by sonication for 1 min over ice bath to form a secondary water-in-oil-in-water emulsion. The emulsion was stirred using a magnetic stirrer, and 5 mL of aqueous calcium chloride solution (60% w/v) was added gradually to the above emulsion. The emulsion was stirred further at ambient conditions for ~18 h and then under vacuum for 1 h to evaporate methylene chloride. For preparing drug-loaded nanoparticles, drug (5–15 mg) was dissolved in the aqueous alginate solution by sonication, which was then processed as above. Nanoparticles formed were recovered by ultracentrifugation (Beckman, Palo Alto, CA) at 145,000g, washed two times with deionized water to remove PVA and untrapped drug, resuspended in water, and lyophilized.

#### *Determination of Drug Loading and Encapsulation Efficiency*

Drug loading in nanoparticles was determined by extracting 5 mg of nanoparticles in 5 mL of alcohol for 30 min and analyzing the alcohol extract for drug content. Methylene blue was quantified by spectrophotometry at 630 nm (Vmax, Molecular devices, CA); rhodamine and fluorescein were determined by fluorescence spectroscopy (excitation/emission wavelengths of 485/528 nm and 494/518 nm, respectively; FLX 8000, Bio-Tek<sup>®</sup>

Instruments, Winooski, VT). All the other drugs were determined by HPLC (see below). Drug loading was defined as the amount of drug encapsulated in 100 mg of nanoparticles, and was represented as % w/w. Drug encapsulation efficiency was expressed as the percent of the total drug added that was encapsulated in nanoparticles.

#### **Determination of Residual Solvent Content**

According to USP29-NF24, methylene chloride is a Class 2 residual solvent, and its concentration in products is limited to 600 ppm. Residual methylene chloride content in selected nanoparticle formulations was determined by USP-NF organic volatile impurities (OVI) Method IV Testing by a commercial testing laboratory (Microbac Laboratories, Inc., Southern Testing & Research Division, Wilson, NC). The data was presented as ppm residual methylene chloride in nanoparticles.

#### **Determination of Particle Size and Zeta potential**

Particle size of nanoparticles was determined by atomic force microscopy (AFM) in the tapping mode and by transmission electron microscopy (TEM). For AFM, silicon tapping tips (TESP, VEECO) were used with a nominal tip radius less than 10 nm as provided by the manufacturer. Nanoparticles were dispersed in deionized water at 1 mg/mL concentration. A droplet of the nanoparticle suspension was then placed on a polyethyleneimine-coated glass coverslip and air dried. Nanoparticles were then imaged using Nanoscope III (Digital Instruments/VEECO) with an E scanner (maximum scan area =  $14.2 \times 14.2 \mu\text{m}^2$ ). The scan rate is 1 Hz and the integral and proportional gains are approximately 0.4 and 0.7, respectively. Height images were plane-fit in the fast scan direction with no additional image filtering. TEM of nanoparticles was performed following negative staining with uranyl acetate. A drop of nanoparticle suspension (1 mg/mL) was placed on Formvar<sup>®</sup>-coated copper grids (Ted Pella, Inc., Redding, CA) and allowed to equilibrate. Excess liquid was removed with a filter paper and a drop of 2% w/v uranyl acetate was added to the grid. After 3 min incubation at room temperature, excess liquid was removed and the grid was air-dried. The dried grid containing the nanoparticles was visualized using a transmission electron microscope (TEM; Philips/FEI, Inc., Briarcliff Manor, NY). The diameters of at least

fifty individual nanoparticles in the TEM images were determined manually using a digital caliper, and was used to calculate the number-average particle size.

Zeta potential was determined using dynamic light scattering. Brookhaven 90Plus zeta potential equipment (Brookhaven instruments, Holtsville, NY) was used. About 1 mg of nanoparticles was dispersed in 1 mL of distilled water by sonication, and was subjected to zeta potential analysis.

#### **In Vitro Release Studies**

*In vitro* release of nanoparticle-encapsulated drug was determined under sink condition (volume of release medium used was enough to dissolve at least four times the quantity of drug present in nanoparticles). Nanoparticles (~5 mg) were dispersed in 0.5 mL of phosphate-buffered saline (PBS, pH 7.4, 0.15M) or in deionized water containing different concentrations of sodium chloride and suspended in DispoDialyzer<sup>®</sup> (10 kDa MWCO, Pierce) dialysis tubes. The dialysis tubes did not retain free drug. These were then placed in a 15-mL centrifuge tube containing 10 mL of the release medium. The whole assembly was shaken at 100 rpm and  $37.0 \pm 0.5^\circ\text{C}$  in an orbital shaker (Brunswick Scientific, C24 incubator shaker, NJ). At predetermined time intervals, 0.5 mL of the release medium was removed from the centrifuge tube, and was replaced with fresh medium. Drug concentration in the release samples was determined as in drug loading determinations. Stability of different drugs under *in vitro* release conditions was determined and the drug release profile was corrected for degradation, if any.

#### **HPLC Analysis**

A Beckman Coulter HPLC system with System Gold<sup>®</sup> 125 solvent module and System Gold<sup>®</sup> 508 autoinjector connected to System Gold<sup>®</sup> 168 PDA detector and Linear Fluor LC 305 fluorescence detector (Altech) were used. A Beckman<sup>®</sup> C-18 (Ultrasphere) column (ODS 4.6 mm  $\times$  250 mm) was used. The following mobile phase compositions and detector wavelengths were used.

*Doxorubicin*: Acetonitrile:water (adjusted to pH 3 with glacial acetic acid) (70:30) at a flow-rate of 1 mL/min; fluorescence detector at 505/550 nm wavelengths. Retention time—7 min.

*Verapamil*: Acetonitrile:sodium acetate (20 mM; pH 4—adjusted with glacial acetic acid):tetrabutylammonium bromide (1.5 mM) (50:20:30) at

flow-rate of 1 mL/min; fluorescence detector at 275/310 nm wavelengths. Retention time—3.8 minutes.

**Clonidine:** Methanol:sodium 1-heptane-sulfonate (0.01M; pH 3—adjusted with glacial acetic acid) (50:50) at a flow-rate of 1 mL/minute; PDA detector at 220 nm. Retention time—8.0 min.

**Diclofenac:** Acetonitrile:sodium acetate (20 mM, pH 4): tetrabutylammonium bromide (1.5 mM) (6:1.6:2.4 ratio) at flow-rate of 1 mL/min; PDA detector at 280 nm. Retention time—6 minutes.

## RESULTS AND DISCUSSION

Alginates are naturally occurring, random, anionic, linear polymers consisting of varying ratios of guluronic and mannuronic acid units (Fig. 1A). Alginate delivery systems are formed when monovalent, water-soluble, salts of guluronic, and mannuronic acid residues undergo aqueous sol-gel transformation to water-insoluble salts

(Fig. 1B) due to the addition of divalent ions such as calcium.<sup>23,24</sup> Alginate polymers have been widely used in biomedical applications as they are biodegradable and biocompatible, but suffer from the limitation of rapid drug release in physiologic salt concentration.<sup>25</sup> In the presence of monovalent (e.g., sodium) salts, insoluble calcium alginate gets converted into soluble form (sodium alginate, for example), resulting in rapid disintegration of the delivery system and drug release.<sup>25</sup> We rationalized that introduction of stronger acid groups in alginate nanoparticles will result in stronger cross-linking and drug-matrix interaction, resulting in enhanced drug encapsulation and sustained release of the encapsulated drug. Based on this rationale, we developed a surfactant-polymer system composed of alginate and anionic surfactant AOT. AOT has a sulfonic group ( $pK_a < 1$ ) in its polar sulfosuccinate head group with a large and branching hydrocarbon tail group (Fig. 1C). AOT forms reverse micelles in nonpolar solvents such as methylene chloride, and

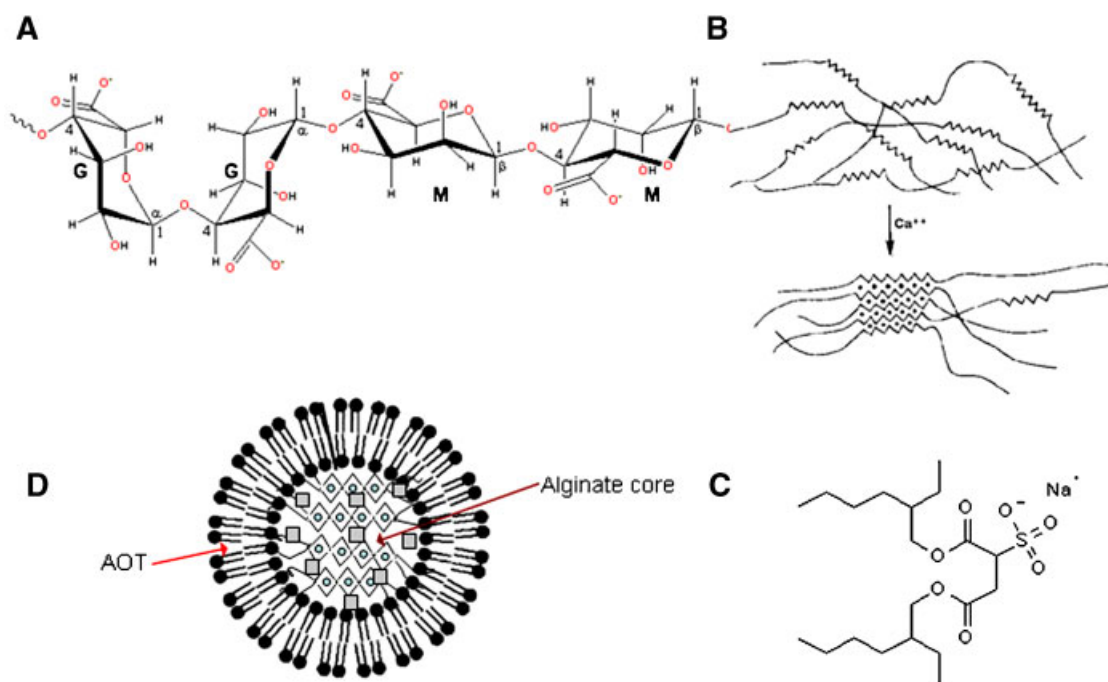


**Figure 1.** (A) Structure of alginate. Alginates are linear unbranched polymers containing  $\beta$ -(1  $\rightarrow$  4)-linked D-mannuronic acid (**M**) and  $\alpha$ -(1  $\rightarrow$  4)-linked L-guluronic acid (**G**) residues. Alginates are not random copolymers but, according to the source algae, consist of blocks of similar and strictly alternating residues (i.e., **MMMMMM**, **GGGGGG**, and **GMGMGMGM**) (B) Crosslinking and 'egg-box' formation of alginate in the presence of calcium salts (C) Structure of AOT shows the sulfosuccinate head group and hydrocarbon tail group (D) Proposed structure of AOT-alginate nanoparticles. Inner core consists of alginate, surrounded by one or more bilayers composed of AOT. Gray squares represent drug molecules. Figures not drawn to scale

because AOT is a double chain amphiphile, it is expected to form a bilayer structure in multiple emulsion.<sup>26</sup> Based on the above property and the multiple emulsion process used, nanoparticles are expected to have a calcium-crosslinked core composed of alginate and AOT head groups, surrounded by a hydrophobic matrix composed of AOT tails, with the drug of interest encapsulated in the core (Fig. 1D).

### Particle Size and Morphology of Nanoparticles

Nanoparticle size was determined by AFM and TEM. For AFM, at least 50 particles from different spots were measured in order to determine the number-average particle size and the standard deviation. Particle diameters in the lateral and vertical dimensions were measured using the sectional analysis tool of the Nanoscope 5.12b48

software. Figure 2A shows representative nanoparticles that are spherical in shape. The average diameter in the lateral direction was measured to be  $79 \text{ nm} \pm 7 \text{ nm}$  while the average vertical diameter was  $28 \text{ nm} \pm 6 \text{ nm}$ . It is expected that polymeric particles are flattened when they are deposited on a surface. In addition, the lateral measurement by AFM includes the projected AFM tip size, which may add up to 20 nm to the actual diameter in the case of the TESP tip. TEM studies also indicated spherical shape of nanoparticles (Fig. 2B). The average diameter of nanoparticles as visualized by TEM was  $38 \text{ nm} \pm 8 \text{ nm}$ , and correlates well with the particle size range determined by AFM.

Particle size is often used to characterize nanoparticles, because it facilitates the understanding of the dispersion and aggregation processes. Further, particle size affects biological handling of nanoparticles.<sup>27</sup> The subhundred

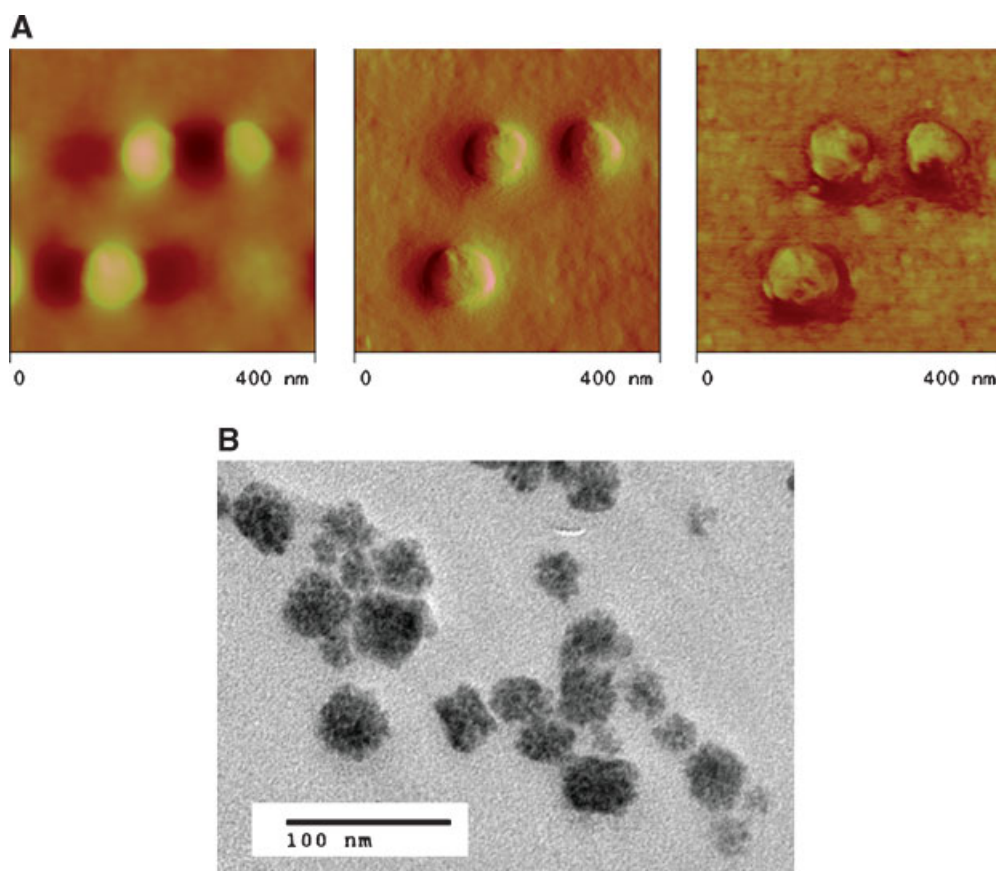


**Figure 2.** (A) AFM images of AOT-alginate nanoparticles in the tapping mode in air. The images from left to right are height, amplitude, and phase images of a representative sample spot with the z-scale of 50 nm, 0.10 V, and  $70^\circ$ , respectively. The scan size is  $400 \times 400 \text{ nm}^2$ . (B) TEM image of AOT-alginate nanoparticles following negative staining with 2% w/v uranyl acetate ( $200,000\times$  magnification).

**Table 1.** Effect of Sodium Alginate Concentration on Methylene Blue Encapsulation<sup>a</sup>

Concentration (% w/v)	Drug Loading (% w/w)	Encapsulation Efficiency (%)	Zeta Potential (mV)
0.1	0.63 ± 0.01	76.4 ± 0.8	-30.5 ± 0.7
0.3	0.63 ± 0.01	76.2 ± 0.8	-34.5 ± 0.9
0.5	0.65 ± 0.01	76.8 ± 0.2	-36.0 ± 1.1
0.7	0.68 ± 0.01	83.0 ± 1.3	-26.1 ± 2.5
1.0	0.82 ± 0.01	99.8 ± 0.6	-36.1 ± 2.1

<sup>a</sup>AOT and PVA concentrations were 20 and 2% w/v, respectively.

nanometer particle size is beneficial in drug delivery, because nanoparticles in this size range have been shown to have higher cellular<sup>27</sup> and tissue uptake.<sup>28-30</sup>

The zeta potential of AOT-alginate nanoparticles was in the range of -25 to -35 mV (Tables 1-3). Previous studies have shown that zeta potential affects the intracellular distribution of nanoparticles.<sup>31</sup> Our proposed model for AOT-alginate nanoparticles (Fig. 1D) suggests that only the negative charges present in the core of the nanoparticle matrix (sulfonate in AOT and carboxyl groups in alginate) are involved in electrostatic interactions with weakly basic drug molecules. Thus, negative charges on the surface of nanoparticles could contribute to the negative zeta potential of AOT-alginate nanoparticles.

### Drug Loading and Encapsulation Efficiency

Initial optimization studies were performed with methylene blue. Methylene blue is a photosensitizer that is currently being investigated for photodynamic therapy of various cancers.<sup>32,33</sup> Drug loading and drug encapsulation efficiency in AOT-alginate nanoparticles was dependent on AOT and alginate concentrations. Increasing the sodium alginate concentration from 0.1 to 1% w/v in the formulation resulted in an increase in

methylene blue loading efficiency from about 77 to 99% (Table 1). Similarly, increasing the AOT concentration from 0.05 to 20% in the formulation resulted in an increase in encapsulation efficiency from 17 to 99% (Table 2).

Drug encapsulation efficiency in nanoparticles was also a function of the amount of drug added to the formulation as shown in Table 3. Encapsulation efficiency was 99% when 5 mg of methylene blue was used in nanoparticle formulation whereas the encapsulation efficiency decreased to 74% when 15 mg of methylene blue was used. We studied the effect of oil phase volume on drug loading to determine if higher amounts of drug can be loaded in nanoparticles without the loss of encapsulation efficiency. When the volume of the AOT phase was decreased from 3 mL to 1.5 mL, drug loading increased to about 1.9% w/v, with an encapsulation efficiency of 80% (Table 4). Decreasing the oil phase volume further to 1 mL and AOT concentration to 5% w/v further increased the drug loading to 3.8% w/w, with a drug encapsulation efficiency of ~50%.

The above results could be explained based on the contribution of electrostatic interactions to drug loading in nanoparticles. Increasing the concentration of either alginate or AOT is expected to increase the number of acidic functional groups available for interaction with basic drug, resulting in better drug entrapment in

**Table 2.** Effect of AOT Concentration on Methylene Blue Encapsulation<sup>a</sup>

Concentration (% w/v)	Drug Loading (% w/w)	Encapsulation Efficiency (%)	Zeta Potential (mV)
0.05	5.06 ± 0.24	16.7 ± 0.8	-32.3 ± 0.9
0.1	4.44 ± 0.05	16.8 ± 0.2	-34.5 ± 2.4
5	1.76 ± 0.02	58.2 ± 0.9	-30.9 ± 0.9
10	1.38 ± 0.02	86.9 ± 1.2	-31.7 ± 2.6
20	0.82 ± 0.01	99.8 ± 1.2	-36.1 ± 2.1

<sup>a</sup>Sodium alginate and PVA concentrations were 1 and 2% w/v, respectively.

**Table 3.** Effect of Methylene Blue Amount Added on Methylene Blue Encapsulation<sup>a</sup>

Amount (mg)	Drug Loading (% w/w)	Encapsulation Efficiency (%)	Zeta Potential (mV)
5.0	0.82 ± 0.01	99.8 ± 0.6	-36.1 ± 2.1
7.5	0.67 ± 0.01	82.7 ± 1.1	-32.2 ± 0.9
10.0	0.65 ± 0.01	80.2 ± 1.7	-26.2 ± 0.8
12.5	0.63 ± 0.01	79.0 ± 0.7	-32.2 ± 1.7
15.0	0.60 ± 0.01	74.1 ± 0.2	-34.6 ± 1.7

<sup>a</sup>Alginate, AOT and PVA concentrations were 1, 20 and 2% w/v, respectively.

**Table 4.** Effect of AOT Volume Fraction on Loading and Encapsulation Efficiency of Doxorubicin Hydrochloride<sup>a</sup>

Volume of AOT Phase (mL)	AOT Concentration (% w/v)	Drug Loading (% w/w)	Encapsulation Efficiency (%)
3	20	0.82 ± 0.01	99.8 ± 1.2
1.5	20	1.86 ± 0.01	80.0 ± 0.3
1	5	3.80 ± 0.11	49.3 ± 1.5

<sup>a</sup>Sodium alginate and PVA concentrations were 1 and 2% w/v, respectively.

nanoparticles. As there are a limited number of functional groups in the nanoparticle matrix that are available for electrostatic interactions with the drug, increase in the amount of drug added to the formulation could have resulted in a decrease in drug entrapment efficiency.

In order to further understand the contribution of electrostatic interactions to drug encapsulation, we studied the encapsulation of weakly acidic drugs, fluorescein sodium, and diclofenac sodium, in nanoparticles. Both diclofenac and fluorescein are low molecular weight drugs (Table 5), and are highly water-soluble. The encapsulation efficiencies for fluorescein and diclofenac were low (~6.0%; Table 5), suggesting that electrostatic interaction between the drug and nanoparticle matrix is an important determinant of drug encapsulation efficiency in

AOT-alginate nanoparticles. Because the structure of the different molecules investigated here are different, it is important to note that other interactions (hydrophobic, hydrogen bonding) could have also contributed, to some extent, to the observed differences in encapsulation efficiencies of different drugs.

To confirm that AOT-alginate nanoparticles can be used for the encapsulation of other weakly basic water-soluble drugs, we investigated the encapsulation efficiencies for verapamil, rhodamine, clonidine, and doxorubicin hydrochloride. Under similar formulation conditions, the above drugs could be loaded in nanoparticles at ~4–6% w/w drug loading (Table 5). These studies confirm the general applicability of AOT-alginate nanoparticles for encapsulation of weakly basic, low molecular weight, water-soluble drugs.

**Table 5.** Encapsulation of Different Drugs in AOT-Alginate Nanoparticles<sup>a</sup>\*

Drug	Molecular Weight (Da)	Drug Loading (% w/w)	Encapsulation Efficiency (%)	Residual Methylene Chloride <sup>a</sup>
Rhodamine	380	4.6 ± 0.2	59.7 ± 2.6	4 ppm
Doxorubicin	580	3.8 ± 0.1	49.3 ± 1.5	3 ppm
Verapamil	491	5.9 ± 0.5	76.8 ± 6.8	9 ppm
Clonidine	266	3.6 ± 0.2	45.7 ± 1.9	ND
Fluorescein	332	0.6 ± 0.0	6.9 ± 0.2	ND
Diclofenac	318	0.5 ± 0.0	6.1 ± 0.4	2 ppm

\*Sodium alginate and PVA concentrations were 1 and 2% w/v, respectively. AOT concentration was 5% w/v and phase volume was 1 mL.

<sup>a</sup>ND – not determined.

The drug loading capacity of AOT-alginate nanoparticles is higher than that reported previously for water-soluble drugs in other nanoparticle formulations. For example, gelatin nanoparticles demonstrated a maximum of 3% w/w loading for methotrexate sodium.<sup>18</sup> PLGA nanoparticles demonstrated 0.26% w/w loading for doxorubicin hydrochloride.<sup>34</sup> A maximum of 0.9% w/w loading was obtained for 5-fluorouracil in polycaprolactone nanoparticles.<sup>35</sup>

### Determination of Residual Solvent Content

According to USP29-NF24, methylene chloride is a Class 2 residual solvent, and its concentration in products is limited to 600 ppm. All the nanoparticles tested had very low levels of residual methylene chloride content (Table 5), and passed the 600 ppm limit set by the US Pharmacopeia.

### In Vitro Drug Release Studies

To determine the ability of AOT-alginate nanoparticles to sustain the release of encapsulated drug, we studied the *in vitro* release of verapamil, doxorubicin, and diclofenac from nanoparticles. Initially, stability of these drugs under the release conditions (PBS, pH 7.4 and 37°C) was investigated. Verapamil and diclofenac were stable under those conditions (data not shown), whereas doxorubicin demonstrated biphasic, first-order degradation profile (Fig. 3). Rate constants were determined for the two phases, and were used to

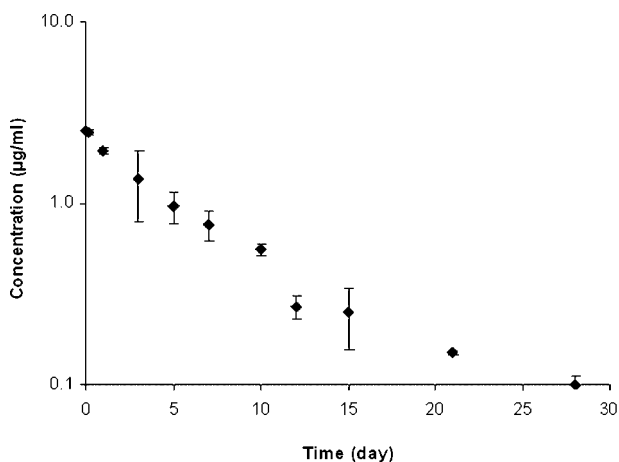


**Figure 3.** Biphasic degradation of doxorubicin in PBS at 37°C and 100 rpm. The  $r^2$  values for the two phases were 0.9890 (1–10 days) and 0.9926 (12–28 days).

correct the *in vitro* release of doxorubicin for degradation. For each time point, cumulative amount of drug released at the previous time point was considered as the initial drug concentration ( $C_0$ ) and the rate constant for degradation ( $k$ ) was used to calculate the new drug concentration ( $C_t$ ) using the first-order rate equation. The amount of drug degraded in the time ( $t$ ) between the previous time point and a particular time point was then calculated using the following equation:

$$\begin{aligned} \text{Amount degraded} &= (C_0 - C_t) = C_0 - C_0 e^{-kt} \\ &= C_0(1 - e^{-kt}) \end{aligned}$$

Nanoparticles demonstrated sustained drug release for both the basic drugs investigated (Fig. 4). For both doxorubicin and verapamil, drug release was near zero-order ( $\sim 45$  and 60% released, respectively;  $r^2$  values of 0.9949 and 0.9977) during the first 15 days, followed by a more sustained drug release, with about 60–70% of the entrapped drug released over a 28-day period.

We also investigated whether AOT-alginate nanoparticles can be used to sustain the release of more than one drug. Nanoparticles were loaded with both verapamil and doxorubicin for this purpose. Doxorubicin, an anticancer agent, is a substrate of the drug efflux transporter P-glycoprotein while verapamil is a competitive inhibitor of P-glycoprotein.<sup>36</sup> Thus, doxorubicin-verapamil combination could potentially be useful for treating drug-resistant cancers. *In vitro* release studies indicate that nanoparticles can

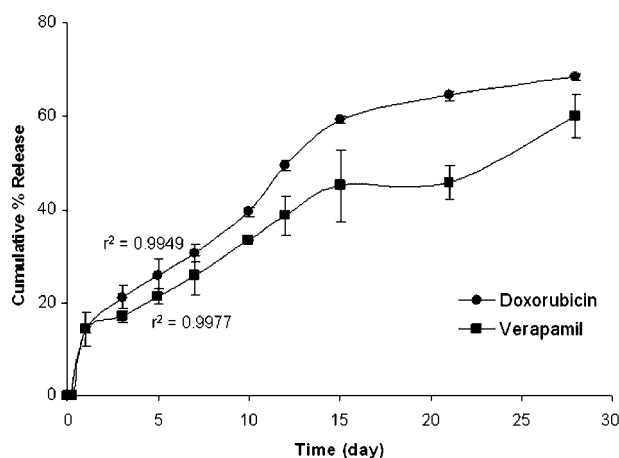


**Figure 4.** *In vitro* release of doxorubicin and verapamil in PBS at 37°C and 100 rpm. Drug loading in nanoparticles was 3.8%, and 1.8% w/w for doxorubicin and verapamil, respectively. The  $r^2$  values shown indicate zero-order drug release between days 1 and 15.

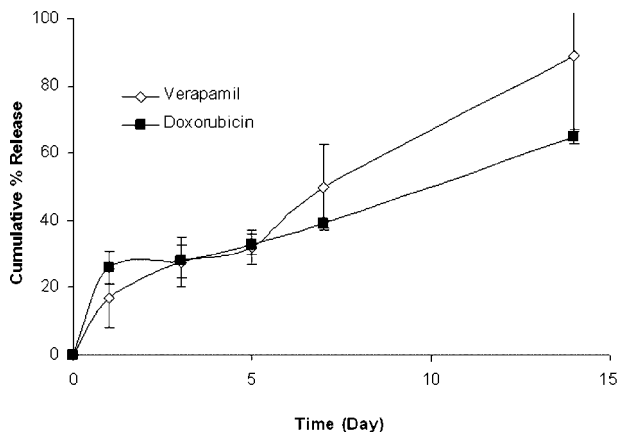


**Figure 5.** Simultaneous *in vitro* release of doxorubicin and verapamil in PBS at 37°C and 100 rpm from nanoparticle formulation loaded with both drugs. Drug loading was 0.4 and 1.4% w/w for doxorubicin and verapamil, respectively.

sustain the release of both drugs (Fig. 5). The release rate of the two drugs, however, was faster from nanoparticles loaded with both the drugs than from nanoparticles loaded with either drug alone.

Previous studies with alginate delivery systems indicate that the main mechanism governing drug release in physiologic fluids is the sodium–calcium exchange.<sup>25</sup> When calcium alginate is introduced in environment rich in monovalent salts (sodium, for example), insoluble calcium alginate is converted into soluble alginate, resulting in solubilization of the delivery system and drug release. In order to determine the contribution of sodium–calcium exchange to drug release, we investigated the effect of sodium ion concentration in the release medium on drug release. As can be seen from Figure 6, increasing the concentration of sodium ions resulted in an increase in rate and extent of drug release from nanoparticles. This strongly suggests that sodium–calcium exchange plays an important role in drug release from nanoparticles. Unlike other alginate systems<sup>25</sup>, AOT-alginate nanoparticles did not rapidly disintegrate in physiological salt solutions, and were stable for more than 3 weeks. Drug release in the absence of sodium ions (0% NaCl; closed triangle; Fig. 6) suggest that other mechanisms such as simple diffusion could also contribute to drug release.

Because electrostatic interactions were found to be important for drug encapsulation, we hypothesized that electrostatic interaction could also influence drug release from nanoparticles. If

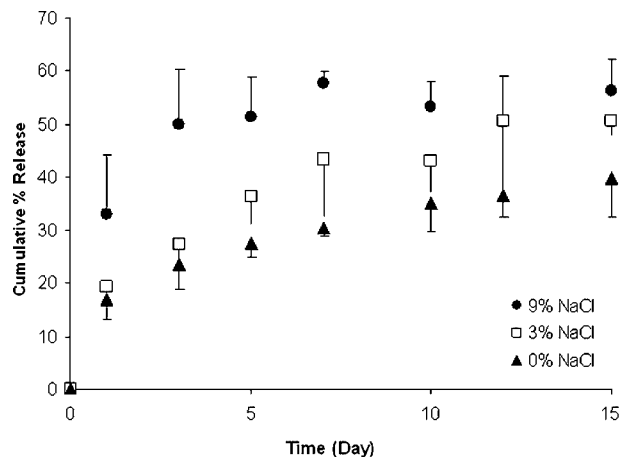


**Figure 6.** Effect of sodium chloride concentration of release medium on *in vitro* release of verapamil. The release was conducted at 37°C and 100 rpm. Verapamil loading in nanoparticles was 1.8% w/w.

electrostatic interactions between basic drug and anionic matrix contribute to sustained drug release, then the release of an acidic drug from nanoparticles can be expected to be faster than that of a basic drug. We investigated the release of diclofenac, a weakly acidic drug, from nanoparticles. As can be seen from Figure 7, release of diclofenac from nanoparticles was faster, with about 70% of the encapsulated drug released in 7 days. This can be compared to about 25–30% release observed for basic drugs in the same time frame.

Our studies thus indicate that electrostatic interaction is an important determinant of drug release. It would be of interest to determine if alginate in nanoparticles could be replaced with other polyanions to obtain similar sustained

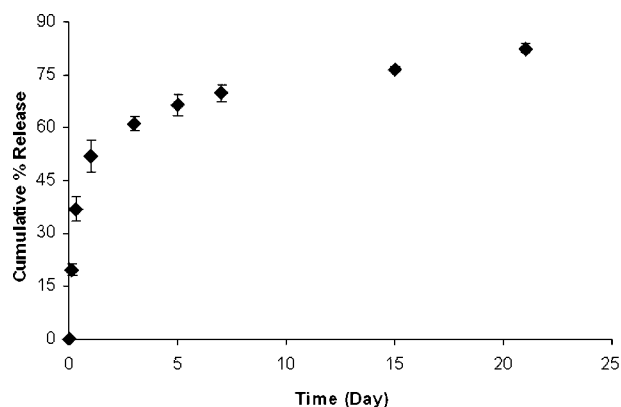


**Figure 7.** *In vitro* release of diclofenac sodium in PBS at 37°C and 100 rpm. Drug loading in nanoparticles was 0.5% w/w.

release properties for weakly basic drugs. A surfactant-polymer system similar to AOT-alginate nanoparticles but composed of basic components (chitosan and a quaternary ammonium surfactant, for example) could be envisioned. Such a system would be potentially useful for acidic drugs.

## CONCLUSION

We have demonstrated efficient encapsulation and sustained release of basic, water-soluble drugs from AOT-alginate nanoparticles. The emulsion-crosslinking technology reported here results in nanoparticles of submicron size and with very low residual methylene chloride content. Drug encapsulation efficiency is dependent on different formulation factors such as alginate, AOT, and drug concentrations. Drug release from nanoparticles appears to be mediated mainly through sodium-calcium exchange as well as electrostatic interaction between drug and nanoparticle matrix. Submicron particle size and sustained release characteristics suggest that surfactant-polymer nanoparticles would be useful for sustained delivery of water-soluble drugs.

## REFERENCES

- Panyam J, Labhasetwar V. 2003. Biodegradable nanoparticles for drug and gene delivery to cells and tissue. *Adv Drug Deliv Rev* 55(3):329–347.
- Calvo P, Gouritin B, Chacun H, Desmaele D, D'Angelo J, Noel JP, Georgin D, Fattal E, Andreux JP, Couvreur P. 2001. Long-circulating PEGylated polycyanoacrylate nanoparticles as new drug carrier for brain delivery. *Pharm Res* 18(8):1157–1166.
- Monsky WL, Fukumura D, Gohongi T, Ancukiewicz M, Weich HA, Torchilin VP, Yuan F, Jain RK. 1999. Augmentation of transvascular transport of macromolecules and nanoparticles in tumors using vascular endothelial growth factor. *Cancer Res* 59(16):4129–4135.
- Stroh M, Zimmer JP, Duda DG, Levchenko TS, Cohen KS, Brown EB, Scadden DT, Torchilin VP, Bawendi MG, Fukumura D, Jain RK. 2005. Quantum dots spectrally distinguish multiple species within the tumor milieu in vivo. *Nat Med* 11(6):678–682.
- Song C, Labhasetwar V, Cui X, Underwood T, Levy RJ. 1998. Arterial uptake of biodegradable nanoparticles for intravascular local drug delivery: results with an acute dog model. *J Control Release* 54(2):201–211.
- Kaul G, Amiji M. 2005. Tumor-targeted gene delivery using poly(ethylene glycol)-modified gelatin nanoparticles: in vitro and in vivo studies. *Pharm Res* 22(6):951–961.
- Oyewumi MO, Mumper RJ. 2003. Influence of formulation parameters on gadolinium entrapment and tumor cell uptake using folate-coated nanoparticles. *Int J Pharm* 251(1–2):85–97.
- Lanza GM, Yu X, Winter PM, Abendschein DR, Karukstis KK, Scott MJ, Chinen LK, Fuhrhop RW, Scherrer DE, Wickline SA. 2002. Targeted antiproliferative drug delivery to vascular smooth muscle cells with a magnetic resonance imaging nanoparticle contrast agent: implications for rational therapy of restenosis. *Circulation* 106(22):2842–2847.
- Panyam J, Williams D, Dash A, Leslie-Pelecky D, Labhasetwar V. 2004. Solid-state solubility influences encapsulation and release of hydrophobic drugs from PLGA/PLA nanoparticles. *J Pharm Sci* 93(7):1804–1814.
- Sahoo SK, Ma W, Labhasetwar V. 2004. Efficacy of transferrin-conjugated paclitaxel-loaded nanoparticles in a murine model of prostate cancer. *Int J Cancer* 112(2):335–340.
- Vauthier C, Dubernet C, Chauvierre C, Brigger I, Couvreur P. 2003. Drug delivery to resistant tumors: the potential of poly(alkyl cyanoacrylate) nanoparticles. *J Control Release* 93(2):151–160.
- Bilati U, Allemann E, Doelker E. 2005. Poly(D,L-lactide-co-glycolide) protein-loaded nanoparticles prepared by the double emulsion method—processing and formulation issues for enhanced entrapment efficiency. *J Microencapsul* 22(2):205–214.
- Leach WT, Simpson DT, Val TN, Anuta EC, Yu Z, Williams RO 3rd, Johnston KP. 2005. Uniform encapsulation of stable protein nanoparticles produced by spray freezing for the reduction of burst release. *J Pharm Sci* 94(1):56–69.
- Prabha S, Labhasetwar V. 2004. Critical determinants in PLGA/PLA nanoparticle-mediated gene expression. *Pharm Res* 21(2):354–364.
- Eroglu H, Kas HS, Oner L, Turkoglu OF, Akalan N, Sargon MF, Ozer N. 2001. The in-vitro and in-vivo characterization of PLGA:L-PLA microspheres containing dexamethasone sodium phosphate. *J Microencapsul* 18(5):603–612.
- Ubrich N, Bouillot P, Pellerin C, Hoffman M, Maincent P. 2004. Preparation and characterization of propranolol hydrochloride nanoparticles: a comparative study. *J Control Release* 97(2):291–300.
- Yi YM, Yang TY, Pan WM. 1999. Preparation and distribution of 5-fluorouracil (125I) sodium alginate-bovine serum albumin nanoparticles. *World J Gastroenterol* 5(1):57–60.
- Cascone MG, Lazzeri L, Carmignani C, Zhu Z. 2002. Gelatin nanoparticles produced by a simple W/O

- emulsion as delivery system for methotrexate. *J Mater Sci Mater Med* 13(5):523–526.
19. Vandervoort J, Ludwig A. 2004. Preparation and evaluation of drug-loaded gelatin nanoparticles for topical ophthalmic use. *Eur J Pharm Biopharm* 57(2):251–261.
  20. Pasparakis G, Bouropoulos N. 2006. Swelling studies and in vitro release of verapamil from calcium alginate and calcium alginate-chitosan beads. *Int J Pharm* 323(1–2):34–42.
  21. Iskakov RM, Kikuchi A, Okano T. 2002. Time-programmed pulsatile release of dextran from calcium-alginate gel beads coated with carboxy-n-propylacrylamide copolymers. *J Control Release* 80(1–3): 57–68.
  22. Shimizu T, Yamato M, Kikuchi A, Okano T. 2003. Cell sheet engineering for myocardial tissue reconstruction. *Biomaterials* 24(13):2309–2316.
  23. Gombotz WR, Yee S. 1998. Protein release from alginate matrices. *Adv Drug Deliv Rev* 31(3): 267–285.
  24. Skaugrud O, Hagen A, Borgersen B, Dornish M. 1999. Biomedical and pharmaceutical applications of alginate and chitosan. *Biotechnol Bioeng* 16: 23–40.
  25. De S, Robinson DH. 2003. Polymer relationships during preparation of chitosan-alginate and poly-L-lysine-alginate nanospheres. *J Control Release* 89(1):101–112.
  26. Israelachvili J. 1991. *Intermolecular and Surface Forces*. 2nd ed. London: Academic Press.
  27. Desai MP, Labhasetwar V, Walter E, Levy RJ, Amidon GL. 1997. The mechanism of uptake of biodegradable microparticles in Caco-2 cells is size dependent. *Pharm Res* 14(11):1568–1573.
  28. Hillyer JF, Albrecht RM. 2001. Gastrointestinal persorption and tissue distribution of differently sized colloidal gold nanoparticles. *J Pharm Sci* 90(12):1927–1936.
  29. Brooking J, Davis SS, Illum L. 2001. Transport of nanoparticles across the rat nasal mucosa. *J Drug Target* 9:267–279.
  30. Florence AT, Hillery AM, Hussain N, Jani PU. 1995. Factors affecting the oral uptake and translocation of polystyrene nanoparticles: histological and analytical evidence. *J Drug Target* 3:65–70.
  31. Panyam J, Zhou WZ, Prabha S, Sahoo SK, Labhasetwar V. 2002. Rapid endo-lysosomal escape of poly(DL-lactide-co-glycolide) nanoparticles: implications for drug and gene delivery. *Faseb J* 16(10):1217–1226.
  32. Serksen SR, Westcott SL, Halas NJ, West JL. 2000. Temperature-sensitive polymer-nanoshell composites for photothermally modulated drug delivery. *J Biomed Mater Res* 51(3):293–298.
  33. Tang W, Xu H, Kopelman R, Philbert MA. 2005. Photodynamic characterization and in vitro application of methylene blue-containing nanoparticle platforms. *Photochem Photobiol* 81(2):242–249.
  34. Yoo HS, Oh JE, Lee KH, Park TG. 1999. Biodegradable nanoparticles containing doxorubicin-PLGA conjugate for sustained release. *Pharm Res* 16(7): 1114–1118.
  35. McCarron PA, Woolfson AD, Keating SM. 2000. Sustained release of 5-fluorouracil from polymeric nanoparticles. *J Pharm Pharmacol* 52(12):1451–1459.
  36. Hendrikse NH. 2000. Monitoring interactions at ATP-dependent drug efflux pumps. *Curr Pharm Des* 6(16):1653–1668.